Momentum dependence of fluorine *K*-edge core exciton in LiF

K. Hämäläinen, S. Galambosi, and J. A. Soininen
Division of X-Ray Physics, Department of Physical Sciences, P.O. Box 64, FIN-00014 University of Helsinki, Finland

Eric L. Shirley
Optical Technology Division, Physics Laboratory, National Institute of Standards and Technology, Gaithersburg, Maryland 20899

J.-P. Rueff and A. Shukla
European Synchrotron Research Facility, Bolte Postale 220, F-38043 Grenoble, France
(Received 29 October 2001; revised manuscript received 22 January 2002; published 29 March 2002)

Nonresonant inelastic x-ray scattering spectra have been measured with an energy loss close to the fluorine *K* edge of lithium fluoride. The extracted dynamic structure factor is well reproduced by a first-principles computational scheme that takes the electron-hole interaction into account. A systematic study of the momentum-transfer dependence with high energy resolution in the close vicinity of the *K* edge shows clear deviations from the dipole approximation. With the help of the calculations, it is shown that the observed deviations are because of an *s*-type exciton.

DOI: 10.1103/PhysRevB.65.155111 PACS number(s): 78.70.Ck, 71.15.−m, 71.35.−y

I. INTRODUCTION

We have studied the nonresonant inelastic x-ray scattering (NRIXS) spectrum of lithium fluoride near the fluorine *K* edge, using both experimental and theoretical methods. LiF is a wide-gap insulator with strong excitonic effects both for the x-ray edge and valence excitations. Dispersion of the valence excitons has been studied both with NRIXS[1–3] and electron energy-loss spectroscopy (EELS).[4,5] The momentum-transfer dependence of the Li *K*-edge exciton has also attracted attention.[3,5] Furthermore, x-ray absorption near-edge structure (XANES) measurements of the fluorine *K* edge in LiF had strong peaks that were associated with excitons.[6]

Inelastic scattering measurements can be accomplished using either photons (NRIXS) or electrons (EELS). The latter has several advantages including higher intensities even when compared with photon fluxes obtainable from third-generation synchrotron sources. However, the resolution and counting statistics obtainable with NRIXS have dramatically improved. Furthermore, two relative merits of NRIXS are the facts that hard x rays are not surface sensitive, and that problems related to multiple scattering are less severe. One of the general advantages of using inelastic scattering methods in the study of x-ray absorption near-edge structures is that both the *magnitude* and the *direction* of the momentum transfer **q** can be used to select the symmetry of the final state of the electron system. In the low-momentum-transfer region, the main contribution to experimental spectra originates from the dipole-allowed transitions, and the only difference compared to x-ray absorption is that in this case the polarization vector **e** is replaced with the momentum transfer **q**.[7] By varying the direction of the momentum-transfer vector, NRIXS can be used to study the anisotropy of the XANES (see, for example, Ref. 8). The magnitude of **q** can be used to distinguish the various core excitations with different spatial symmetries.[3,5,9]

Although there have been advances in the theoretical understanding of excited states in solids in recent years, XANES is still not completely understood from the theoretical point of view. When an inelastic scattering process from an inner-shell occurs, an electron is excited and a core hole is created. Several first-principles schemes have been suggested to treat the core hole-electron interaction.[10,11] The problem is rather complicated, because the excited electron interacts with both the core hole and the polarization cloud created by the core hole, as well as with its own polarization cloud. In this work we have used a first-principles[12–14] calculation scheme that was recently developed to model these interactions and their effect in NRIXS.

In the following, we will first give a short description of both the theoretical background of NRIXS and the calculation scheme and describe the experimental setup. We will then present our results and discuss their relevance. Finally, some conclusions will be drawn.

II. THEORY

In a nonresonant inelastic x-ray scattering experiment a double-differential cross section $d^2\sigma/d\Omega d\omega$ is measured. The nonrelativistic interaction Hamiltonian for the electron-photon system is

$$\mathbf{H}_{e-p}=\sum_i \left[\frac{\alpha^2}{2}\mathbf{A}(\mathbf{r}_i)\cdot\mathbf{A}(\mathbf{r}_i)+\alpha\mathbf{p}_i\cdot\mathbf{A}(\mathbf{r}_i)\right], \qquad (1)$$

where **A** is the photon vector field operator, the index *i* refers to the *i*th electron of the system, and α is the fine-structure constant. Within a first-order perturbation-theory treatment, only the $\mathbf{A}\cdot\mathbf{A}$ term in Eq. (1) contributes to the scattering cross section. The $\mathbf{p}\cdot\mathbf{A}$ term contributes to scattering in the second order, albeit at the same order in α, i.e., α^2. However, because the incident photon energy is far from a resonance, this term is not relevant in our case (the corresponding spectral features are located at a different energy region). In this

case the differential cross section for NRIXS is related to the dynamic structure factor $S(\mathbf{q},\omega)$ of the electron system by

$$\frac{d^2\sigma}{d\Omega d\omega}=\left(\frac{d\sigma}{d\Omega}\right)_{\mathrm{Th}} S(\mathbf{q},\omega), \tag{2}$$

where $(d\sigma/d\Omega)_{\mathrm{Th}}$ is the Thomson scattering cross section. The dynamic structure factor depends only on the momentum ($\mathbf{q}$) and energy (ω) transferred from the scattering photon to the system. The dynamic structure factor is

$$S(\mathbf{q},\omega)=\sum_F |\langle F|\hat{\rho}_{\mathbf{q}}^{\dagger}|I\rangle|^2 \delta(E_F-E_I-\omega), \tag{3}$$

where $|F\rangle$ is the final and $|I\rangle$ the initial electronic state with energies of E_F and E_I, respectively. The operator $\hat{\rho}_{\mathbf{q}}^{\dagger}$ is a Fourier transform of the electron-density operator. In the second-quantized form $\hat{\rho}_{\mathbf{q}}^{\dagger}$ can be written as

$$\hat{\rho}_{\mathbf{q}}^{\dagger}=\sum_{ij} \langle \phi_i|e^{i\mathbf{q}\cdot\mathbf{r}}|\phi_j\rangle \hat{a}_i^{\dagger}\hat{a}_j, \tag{4}$$

where ϕ_i and ϕ_j are single-particle states and $\hat{a}_i^{\dagger}$ ($\hat{a}_i$) is the corresponding creation (annihilation) operator. The advantage of NRIXS (and other probes based on inelastic scattering) in studying excitations from atomiclike states with a well defined lm can be seen if the exponential in Eq. (4) is expanded using the familiar form $\exp(i\mathbf{q}\cdot\mathbf{r})=1+i\mathbf{q}\cdot\mathbf{r}+(i\mathbf{q}\cdot\mathbf{r})^2/2+\cdots$. The first term to contribute in this expansion is $i\mathbf{q}\cdot\mathbf{r}$, that gives rise to dipole-allowed ($\Delta l=\pm 1$) excitations in NRIXS. The dipole-allowed transitions are dominant in the low-momentum-transfer region, and when the momentum transfer is increased the other channels (for example, $\Delta l=0$) gain spectral weight. This can be used to study the spatial symmetries of core excitations as was done in Refs. 5 and 9. In this work we use this property of NRIXS to study the symmetry of core excitons near the fluorine K edge in LiF.

By assuming completeness of the final states, Eq. (3) can be rewritten

$$S(\mathbf{q},\omega)=-\frac{1}{\pi}\lim_{\eta\to 0}\mathrm{Im}\langle I|\hat{\rho}_{\mathbf{q}}\frac{1}{\omega+E_I-\hat{H}+i\eta}\hat{\rho}_{\mathbf{q}}^{\dagger}|I\rangle, \tag{5}$$

where $\hat{H}$ is the full many-body final-state Hamiltonian. In the current calculation scheme,[13] this is approximated by

$$S(\mathbf{q},\omega)=-\frac{1}{\pi}\mathrm{Im}\langle 0|\hat{\rho}_{\mathbf{q}}\frac{1}{\omega-\hat{H}_{eff}+i\gamma(\omega)}\hat{\rho}_{\mathbf{q}}^{\dagger}|0\rangle, \tag{6}$$

where $\hat{H}_{eff}$ is an approximate model Hamiltonian for the excited state. The initial state of the system ($|I\rangle$) is approximated by a single-determinant ground state $|0\rangle$. The finite parameter $\gamma(\omega)$ accounts for the lifetime broadening of the spectrum. The effective Hamiltonian,

$$\hat{H}_{eff}=\hat{H}_0+V_d+V_x,$$

includes a single-particle term ($\hat{H}_0$, accounting for the electron and the core hole), and two electron-hole interaction terms: a screened Coulomb interaction V_d between the core hole and the electron and a bare exchange interaction V_x. As explained in Ref. 13, the excited state is expanded using a basis of core hole-electron pair wave functions. In this case, $\hat{H}_0$ is a diagonal matrix, with its diagonal matrix elements being the difference between the energy of the hole and the electron single-particle states.

The single-particle conduction-band states were calculated using the local-density approximation,[15,16] with the exchange-correlation function of Ceperley and Alder[17] as parametrized by Perdew and Zunger.[18] This was done in a plane-wave pseudopotential framework, using codes capable of calculations discussed in Refs. 19, which are maintained by ourselves and described further in Refs. 20 and 21. The core states were calculated using an atomic Hartree-Fock code written by ourselves.[22] The matrix elements for V_x and $\hat{\rho}_{\mathbf{q}}^{\dagger}$ depend on the spatial overlap of the conduction band and core states. For these matrix elements we use a pseudopotential-inversion scheme[23,24] to correct for the errors originating from using conduction-band-states wave functions obtained from pseudopotential calculations. (Such wave functions are normalized correctly, but have fewer radial nodes in the core regions of atoms.)

In the quantitative comparison of calculated results with the measurements, it is important to have estimates for the accuracy of the theoretical spectra. The error coming from the shortcomings of the theoretical approximations can be most easily estimated by comparing the calculated result with the experiment, whereas the numerical convergence of the present results is substantially better than the level of disagreement with the experiment. We used Vanderbilt pseudopotentials[25] with a plane-wave cutoff of 100 Ry. The experimental lattice constant of 4.02 Å was used in the calculation and sampling of 4096 k points in the first Brillouin zone was found to give a converged result. For the computation of spectra up to 10 eV above the fluorine K edge, 30 conduction bands (corresponding to a 75-eV energy range) were used. For spectra up to 60 eV above the edge, we used 50 conduction bands (corresponding to a 105-eV energy range). All of the above numerical cutoffs were confirmed to be inconsequential for the current results in this study and in previous studies of LiF. The lifetime broadening parameter $\gamma(\omega)$ is approximated by dividing it into two parts. The first one is energy-independent and is because of the natural linewidth of a fluorine K shell hole (0.24 eV). The second part is the electron lifetime, and it is energy-dependent. We calculate it within the so-called "GW approximation,"[26] using a generalized plasmon-pole model and a model dielectric function.[27,28]

III. EXPERIMENT

The experiment was performed at the beamline ID16 at the European Synchrotron Radiation Facility. The x rays were produced by two consecutive undulators and monochromatized using a cryogenically cooled double-crystal

monochromator utilizing the Si (111) reflections. The scattered photons were analyzed using a spherically bent Si (111) crystal as well within a Rowland-circle geometry with a bending radius of 1 m. The diameter of the analyzer crystal was 96 mm, but the active area of the crystal was limited to 60 mm of diameter in order to improve the energy resolution and to limit the spread of scattering angles, which dominates the momentum resolution.

The energy-transfer scans were performed utilizing the so-called inverse-energy scan technique,[29,30] i.e., keeping the scattered energy fixed (corresponding to a fixed analyzer Bragg angle of 86° while tuning the incident energy). Furthermore, the undulator gaps were moved synchronously to guarantee the maximum photon flux as well as a constant beam profile on the sample. The extended energy range measurements where the extreme energy resolution was not crucial were performed using the Si (111) premonochromator only and the Si (555) reflection at the fixed scattered energy of 9.912 keV. The total energy resolution of 1.9 eV was determined from the full width at half maximum (FWHM) of the quasielastic line.

The energy scans within 20 eV around the fluorine *K* edge were performed with a somewhat higher energy resolution in order to study this part of the spectra in more detail. The higher energy resolution was achieved by inserting an additional channel-cut monochromator between the sample and the premonochromator. The channel-cut crystal utilized the Si (400) reflection. For this setup a Si (444) analyzer was used at the fixed scattered energy of 7.920 keV and the energy resolution was improved to 1.0 eV FWHM.

The absolute value of the momentum transfer q depends on the scattering angle 2θ, incident energy ω_1 and scattered energy ω_2 as $q^2 \propto \omega_1^2 + \omega_2^2 - 2\omega_1\omega_2 \cos 2\theta$. The measurements were carried out in the horizontal scattering plane. Because of the linear polarization of the incident radiation, this somewhat limits the available scattering angles in the vicinity of 90° because of a dramatic intensity loss. Because the incident energy was tuned less than 1% during the scans, the momentum transfer can be regarded as a constant within this energy-transfer range. The momentum-transfer resolution was dominated by the finite size of the analyzer crystal, and the relative momentum-transfer resolution $\Delta q/q$ varied between 0.22 at $q = 2.72$ Å^{-1} to 0.01 at $q = 10.2$ Å^{-1}.

A single-crystal LiF sample with a size of 25 mm $\times$10 mm$\times$0.4 mm was used in the experiment. The orientation of the sample was determined using the Laue technique, and it was found that the faces of the crystal coincided with the faces of the LiF conventional cubic unit cell. Low absorption, because of the thin sample, made it possible to collect the data even in a transmission geometry. Large-scattering-angle measurements were performed in a symmetric reflection geometry, while for smaller angles, the symmetric transmission configuration was used. Within all measurements the direction of the momentum transfer was kept fixed along the (100) direction of the conventional unit cell, while the absolute value of q was varied by changing the scattering angle. Vacuum chambers were utilized in the path of the x rays in order to reduce the air absorption and the air scattering. The measured spectra were corrected for all the energy-dependent experimental factors, such as beam monitor efficiency, air and Kapton-window absorption, and the sample self-absorption. However, all of these change only by a few percent over the energy range of interest close to the fluorine *K* edge. For each momentum-transfer value several scans were collected in order to check the data consistency and errors related to incident intensity normalization, beam movements, sample deterioration, etc. Individual scans were found to be identical within the counting statistics. Therefore, the statistical error bars indicated in the figures should reflect the total experimental standard uncertainty.

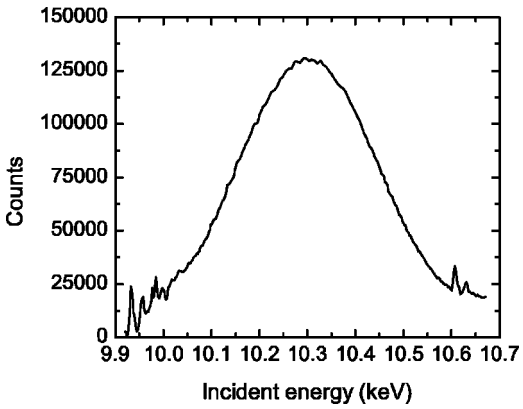

FIG. 1. The measured inelastic scattering cross section over an extended energy-transfer range. The various inelastic scattering features are discussed in the text. The experiment was performed by scanning the incident photon energy and keeping the scattered photon energy fixed at 9.912 keV (elastic line is not shown in the figure). Uncertainties of the data would be miniscule on the scale plotted.

Figure 1 shows a typical energy-loss spectrum over an extended energy region measured at the scattering angle of 160° and fixed scattered energy of 9.912 keV. Various distinct inelastic contributions are visible in the spectrum: the valence excitations with a few tens of eV energy loss, a broad Compton contribution peaked at around 10.3 keV, and the fluorine *K* edge around 10.6 keV. As can be seen in the figure, the measured fluorine *K*-electron contribution is located on the top of a large background originating from the Compton scattering from all the other electrons in the system. Especially in the large-momentum-transfer region, a careful subtraction of this Compton tail is essential. Therefore, a theoretical Compton profile for LiF was calculated by summing the tabulated profiles for the Li^+ and F^- ions[31] and then the profile was scaled to the experimental data points just below the fluorine *K* edge. Even for the largest-momentum-transfer values, the fluorine *K* edge was located above $p_z \sim 3.8$ Å^{-1}, which is far from the maximum of the Compton peak ($p_z \sim 0$ Å^{-1}). According to previous studies,[32] when considering scattering so far from the maximum of the Compton peak, the simple free-ion Li^+F^- model gives the same scattering intensity distribution to within 2% of more sophisticated calculations, which are in excellent agreement with the experimental results. After the subtraction the remaining fluorine *K*-edge contribution was corrected for the polarization and energy factors in the Thomson

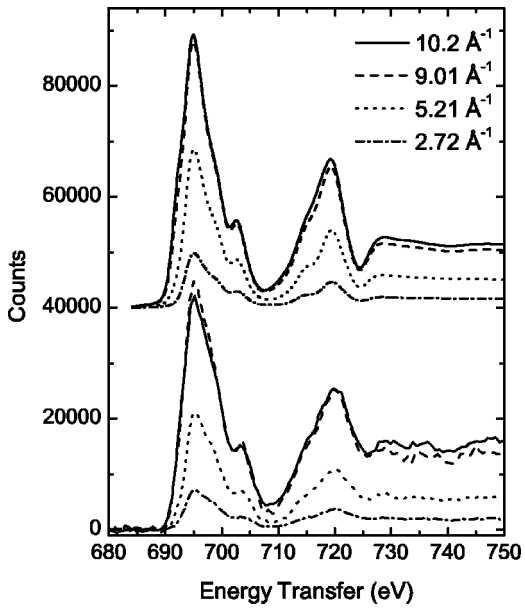

FIG. 2. The experimental (lower) and theoretical (upper) momentum-transfer dependence of $S(\mathbf{q},\omega)$ of LiF over an extended energy-transfer range starting from the fluorine *K* edge. The momentum-transfer values *q* are indicated in the figure. The theoretical spectra have been displaced upwards by 4×10^4 counts for clarity. Uncertainties of the data would be miniscule on the scale plotted.

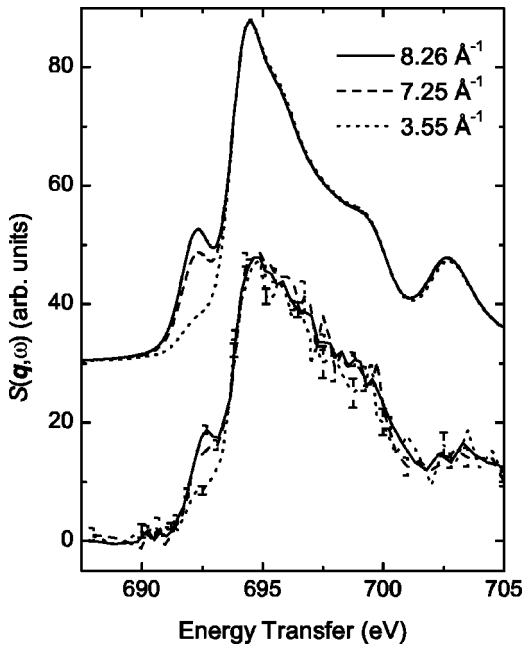

FIG. 3. The experimental (lower) and theoretical (upper) momentum-transfer dependence of the fluorine *K*-edge exciton. The various momentum-transfer values *q* are indicated in the figure. Indicated uncertainties are shown at the one-standard-deviation level. The theoretical spectra are shifted vertically by 30 units for clarity.

cross section. After these corrections the experimental dynamic structure factor follows quite well the expected overall q^2 dependence.

IV. RESULTS AND DISCUSSION

In Fig. 2 both the experimental and the theoretical fluorine *K*-edge NRIXS spectra are presented as a function of energy and momentum transfer. After the experimental corrections described earlier were made, the data were scaled to the theoretical results using a common scaling factor for all experimental data. The complete *f*-sum rule could not be used, because the data do not reach zero rapidly enough. The calculated spectra were convolved with a Gaussian to account for the experimental energy resolution of 1.9 eV FWHM. The overall agreement between experiment and theory is very good. Furthermore, the behavior of the spectra as a function of *q* is also well reproduced with differences only in intensity. The shape of the spectra does not change significantly as a function of momentum transfer, indicating that the primary excitation channels in this energy region are the dipole-allowed excitations from a flat core band. Even for this wide energy and momentum range, the measured inelastic spectra have the same structures as the experimental[6] and calculated x-ray absorption spectra.[13] This demonstrates that NRIXS can be used to study NEXAFS- (near-edge x-ray-absorption fine structure) like excitations even at relatively high-momentum transfers (up to 10.2 Å^{-1} here). This is an important result, because, in certain cases, higher count rates are obtainable in NRIXS at higher momentum transfers.

The main result of this work is presented in Fig 3. The very near-edge structure of the fluorine *K* edge was measured with an energy resolution of about 1.0 eV. The figure shows both the experimental and the theoretical results for three different momentum-transfer values. The calculated spectra were convolved with a 1.0-eV FWHM Gaussian. In this case, the spectra were normalized to have the same area under the curve for the energy transfer values above 694 eV. This was done to emphasize the distinct momentum transfer dependence of the different structures of the spectra. With the improved energy resolution, an exciton peak in the spectra ~ 2 eV below the main *K* edge can be resolved. This rapidly gains weight compared to the rest of the spectrum as the magnitude of the momentum transfer is increased, in both the experimental and theoretical spectra. We attribute this to the q^4 dependence of the *s*-type exciton cross section compared to the usual q^2 dependence of dipole-allowed excitations. Hence, the relative intensity of the *s*-type exciton peak increases as q^2. The spectrum above 694 eV stays almost the same for this momentum-transfer range. When compared with the experimental[6] and calculated[12,13] x-ray absorption spectra, it can be attributed to dipole-allowed excitations.

In Ref. 6 the spatial symmetries of the excited states were studied using different orientations of the polarization vector with respect to the crystal lattice. No anisotropy was observed and Hudson *et al.*[6] concluded that the near-edge structures of the intrinsically small-*q* absorption spectra resulted from excitations with the same or similar spatial symmetry. As discussed earlier, the dipole-allowed transitions behave as q^2 and the next term in the expansion as q^4. From this fact and from the electronic structure of LiF, we can conclude that the peak below the main absorption edge results from

transitions to an *s*-type final state ($\Delta l = 0$). This conclusion was also verified by our theoretical calculations. The agreement between the calculated and the experimental exciton spectra is good, except that the calculations slightly overestimate the weight of the excitonic structures close to the edge.

We have studied the momentum-transfer dependence of the fluorine *K* edge in LiF using nonresonant inelastic x-ray scattering. We were able to conclude from our combined theoretical and experimental study that there is an *s*-type core exciton approximately 2 eV below the absorption edge. Additionally, we were able to study the NEXAFS-like excitations using NRIXS and obtained good agreement with the results of x-ray absorption studies. The overall agreement between experiment and theory over a relatively large energy- and momentum-transfer range was good. The main discrepancy was that the theory slightly overestimated the spectral weight of core excitons, which is suggested, for instance, by the measured and calculated ratios of intensities around 695 eV vs 700 eV in Fig. 3, and by the ratios of the near-edge and high-energy features in Fig. 2.

ACKNOWLEDGMENTS

The authors would like to acknowledge fruitful interactions with W. Caliebe, S. Huotari, C.-C. Kao, M. Krisch, S. Manninen, and F. Sette. This project is supported by the Academy of Finland (Grant No. 7379/39182/40732).

[1] W.A. Caliebe, J.A. Soininen, E.L. Shirley, C.-C. Kao, and K. Hämäläinen, Phys. Rev. Lett. **84**, 3907 (2000).
[2] J.A. Soininen and E.L. Shirley, Phys. Rev. B **61**, 16423 (2000).
[3] W. A. Caliebe, Ph.D. thesis, University of Kiel, 1997.
[4] A. A. Cafolla, Ph.D. thesis, University of Virginia, 1985.
[5] J.R. Fields, P.C. Gibbons, and S.E. Schnatterly, Phys. Rev. Lett. **38**, 430 (1977).
[6] E. Hudson, E. Moler, Y. Zheng, S. Kellar, P. Heimann, Z. Hussain, and D.A. Shirley, Phys. Rev. B **49**, 3701 (1994).
[7] Y. Mizuno and Y. Ohmura, J. Phys. Soc. Jpn. **22**, 445 (1967).
[8] H. Nagasawa, S. Mourikis, and W. Schülke, J. Phys. Soc. Jpn. **58**, 710 (1989).
[9] M.H. Krisch, F. Sette, C. Masciovecchio, and R. Verbeni, Phys. Rev. Lett. **78**, 2843 (1997).
[10] J.J. Rehr and R.C. Alberts, Rev. Mod. Phys. **72**, 621 (2000).
[11] T. Mizoguchi, I. Tanaka, M. Yoshiya, F. Oba, K. Ogasawara, and H. Adachi, Phys. Rev. B **61**, 2180 (2000).
[12] E.L. Shirley, Phys. Rev. Lett. **80**, 794 (1998).
[13] J.A. Soininen and E.L. Shirley, Phys. Rev. B **64**, 165112 (2001).
[14] J.A. Soininen, K. Hämäläinen, W.A. Caliebe, C.-C. Kao, and E.L. Shirley, J. Phys.: Condens. Matter **13**, 8039 (2001).
[15] P. Hohenberg and W. Kohn, Phys. Rev. **136**, 864 (1964).
[16] W. Kohn and L.J. Sham, Phys. Rev. **140**, 1133 (1965).
[17] D.M. Ceperley and B.J. Alder, Phys. Rev. Lett. **45**, 566 (1980).
[18] J. Perdew and A. Zunger, Phys. Rev. B **23**, 5048 (1981).
[19] W.E. Pickett, Comput. Phys. Rep. **9**, 115 (1989).
[20] E.L. Shirley, L.J. Terminello, J.E. Klepeis, and F.J. Himpsel, Phys. Rev. B **53**, 10296 (1996).
[21] E.L. Shirley, Phys. Rev. B **54**, 16464 (1996).
[22] E.L. Shirley, Ph.D. thesis, University of Illinois, 1991.
[23] E.L. Shirley, J. Electron Spectrosc. Relat. Phenom. **110-111**, 305 (2000).
[24] E.L. Shirley, S.I. Merritt, and J.A. Soininen (unpublished).
[25] D. Vanderbilt, Phys. Rev. B **32**, 8412 (1985).
[26] L. Hedin, Phys. Rev. **139**, 796 (1965).
[27] M.S. Hybertsen and S.G. Louie, Phys. Rev. B **37**, 2733 (1988).
[28] Z.H. Levine and S.G. Louie, Phys. Rev. B **25**, 6310 (1982).
[29] W. Schülke and H. Nagasawa, Nucl. Instrum. Methods Phys. Res. A **222**, 203 (1984).
[30] K. Hämäläinen, S. Manninen, C.-C. Kao, W. Caliebe, J.B. Hastings, A. Bansil, S. Kaprzyk, and P.M. Platzman, Phys. Rev. B **54**, 5453 (1996).
[31] F. Biggs, L.B. Mendelsohn, and J.B. Mann, Sandia Laboratories Report No. **SAND75-0636**, 1976 (unpublished).
[32] B. Williams, *Compton Scattering* (McGraw-Hill, New York, 1977).